BNL-200012-2018-JAAM

Study of sub-pixel position resolution with time-correlated transient signals in 3D pixelated CdZnTe detectors with varying pixel sizes

L. Ocampo Giraldo,

To be published in "Nuclear Inst. and Methods in Physics Research, A"

March 2018

Nonproliferation and National Security Department

Brookhaven National Laboratory

U.S. Department of Energy

USDOE National Nuclear Security Administration (NNSA),

USDOE National Nuclear Security Administration (NNSA), Office of Nonproliferation and Verification Research and Development (NA-22)

DISCLAIMER

Study of sub-pixel position resolution with time-correlated transient signals in 3D pixelated CdZnTe detectors with varying pixel sizes

L. Ocampo Giraldo[ab1], A. E. Bolotnikov[b], G. S. Camarda[b], G. De Geronimo[b], J. Fried[b], R. Gul[b], D. Hodges[c], A. Hossain[b], K. Ünlü[a], E. Vernon[b], G. Yang[b], R. B. James[d]

[a]*Pennsylvania State University, University Park, PA, US*
[b]*Brookhaven National Laboratory, Upton, NY, US*
[c]*University of Texas at El Paso, El Paso, TX, US*
[d]*Savannah River National Laboratory, Aiken, SC, US*

***Abstract*— We evaluated the sub-pixel position resolution achievable in large-volume CdZnTe pixelated detectors with conventional pixel patterns and for several different pixel sizes: 2.8-mm, 1.72-mm, 1.4-mm and 0.8-mm. Achieving position resolution below the physical dimensions of pixels (sub-pixel resolution) is a practical path for making high-granularity position-sensitive detectors, < 100 µm, using a limited number of pixels dictated by the mechanical constraints and multi-channel readout electronics. High position sensitivity is important for improving the imaging capability of CZT gamma cameras. It also allows for making more accurate corrections of response non-uniformities caused by crystal defects, thus enabling use of standard-grade (unselected) and less expensive CZT crystals for producing large-volume position-sensitive CZT detectors feasible for many practical applications. We analyzed the digitized charge signals from a representative 9 pixels and the cathode, generated using a pulsed-laser light beam focused down to 10 □m (650 nm) to scan over a selected 3x3 pixel area. We applied our digital pulse processing technique to the time-correlated signals captured from adjacent pixels to achieve and evaluate the capability for sub-pixel position resolution. As an example, we also demonstrated an application of 3D corrections to improve the energy resolution and positional information of the events for the tested detectors.**

Keywords: CdZnTe, High-granularity detectors, 3D pixelated detectors, Crystal defects, Charge sharing, Charge-loss correction

1. Introduction

Large-volume, > 1 cm^3, position-sensitive CdZnTe (CZT) gamma-ray detectors have been proposed and used in many applications [1]. Among them, a 20x20x15 mm^3 3D position-sensitive detector developed by the Orion radiation measurement group at University of Michigan [2] demonstrated a record breaking energy resolution, high detection efficiency and advanced imaging capabilities. However, these kinds of detectors mainly rely on using premium-grade (selected) CZT material, which has a low production yield and high cost. The proliferation of this highly demanded technology is connected to the growing supply of low-cost material free from crystal defects. The steady supply of such material has yet not been achieved. An alternative (and more economical) approach is to employ more accurate charge-loss (or response non-uniformity) correction techniques, which rely on using high-granularity position sensitive detectors. These techniques allow for using standard-grade materials to reduce the device cost without compromising their performance. High position sensitivity allows us to virtually divide the detector active volume into small voxels and equalize the responses from each voxel. Recently, we demonstrated this approach for 3D pixelated detectors with small-pixel sizes, using charge sharing to enhance position resolution [3]. Using the collected-charge signals generated as a result of the charge sharing is an easy and straightforward approach for achieving sub-pixel resolution. However, its main drawback is that it requires using small pixels and readout channels, which makes this approach impractical for many applications due to system complexity and power consumption in the readout ASIC. A more practical approach involves use of the induced signals from the adjacent pixels to refine the position resolution. In this work, we investigated several commercial pixelated detectors with varying pixel sizes using the time-correlated transient signals.

[1]Corresponding author
Postal address: Brookhaven National Laboratory, Upton, NY 11973
E-mail address: lio5000@psu.edu

The approach of using the induced-charge signals from adjacent pixels to refine the position resolution of events was originally proposed (to the best of our knowledge) by Warburton and employed by several researchers [4-8]. It is applied when the whole charge from the electron cloud is collected on a single pixel. In such cases, the electron cloud induces transient signals on neighboring pixels, and the X-Y coordinates of interaction points can be obtained from the amplitudes of the transient signals. Theoretically, this approach should provide a sub-pixel resolution, but only within a geometrical area limited by the size of the electron cloud. In reality, both types of events occur in pixelated detectors with the relative number of shared events increasing with decreasing pixel size. The total charge from the electron cloud can be collected on a single pixel (single-pixel events), or it can be shared among several pixels (charge-sharing events). This means that both approaches should be combined to evaluate the coordinates of the interaction points in pixelated detectors. In most cases, the researchers used a center-of-gravity algorithm to process the amplitudes of the shaped signals. More advanced algorithms have been proposed [9-10] using the signal waveforms and the maximum-likelihood method to find the best fit to the benchmark waveforms obtained from a calibration run or simulated theoretically and analyzing pulse shapes of strip signals.

Recently, we evaluated sub-pixel position resolution of a 3D pixelated detector with a pixel size of 1.72x1.72 mm^2 and demonstrated the advantage of using the time-correlated approach for enhancing the position resolution [11]. This was done considering single-point interaction events only, which were generated by means of a pulsed laser. In this work, we investigated the position resolution of commercial pixelated detectors with standard patterns of varying pixel sizes (0.8-mm, 1.4-mm, 1.72-mm, and 2.85-mm) and illustrate the application of the response corrections in a pixelated detector. In this work we conduct systematic measurements to evaluate the energy dependencies of position resolution (%FWHM) using pixelated detectors with different pixel sizes. These data help to optimize the pixel size for achieving high-energy resolution (after response corrections) of large-volume CZT detectors, while using a minimum number of readout channels and standard (unselected) grade CZT crystals. Furthermore, this work aims to show the improvements in spectral resolution when applying 3D corrections to a pixelated crystal.

2. EXPERIMENTAL SETUP

The pulsed laser beam system is comprised of a 1-mW laser beam (650 nm wavelength) coupled with a single mode optical 9-µm fiber and microscope objective. The beam is manually focused on the surface of the detector over the pixels of interest using the same objective. We note, that the short light pulse (in these measurements we could vary the pulse width in the range 10-100 ns) cannot entirely substitute for actual gamma-ray events, but it has several advantages for the measurements conducted in this study; it provides precise timing and the original location of the injected charge, and ability to generate signals equivalent to gamma rays from a wide energy range (100 keV – 2.5 MeV).

The detector being tested was plugged into the test box's motherboard containing 10 charge-sensitive preamplifiers (eV-5093), whose inputs were connected to the pixels of interest in the detector (3x3 area). The detector system was mounted on the motorized X-Y translation stage controlled by a computer.

The detectors mounted on substrates were acquired from two vendors: Redlen Technologies, Inc. and eV Products, Inc. with a large fraction of working pixels (> 50%) to ensure that we could scan over several 3x3 pixel areas for each detector. The pixel sizes varied from 0.8 mm to 2.85 mm as shown in Table 1. The socket board of the readout detector system allows selecting and reading out the signals from any of the pixels. The signals from the nine pixels and the cathode were recorded using two synchronized oscilloscopes: a LeCroy HDO 8058 oscilloscope and a LeCroy 6050 Waverunner. The charge signals, generated by the electron cloud as it drifted between the cathode and the anode, were sampled at 10-ns time intervals (bins) and stored in the oscilloscopes' memories for further analysis. The measurements were taken at room temperature around 21-22 °C. For the energy calibration, we used a standard ^{137}Cs source. The high-voltage values were 500 volts per 5 mm in height for each detector.

Table 1. Commercial detectors used in these measurements.

Manufacturer	Dimensions (mm^3)	Pixel pattern	Pixel Size (mm)	Nominal Size (mm)	Position resolution at energy corresponding to 662 keV (µm)
eV Products	10x10x10	11x11	0.80	0.50	53.54
eV Products	15x15x5	10x10	1.40	1.12	75.10
Redlen Tech.	20x20x10	11x11	1.72	1.22	109.80
eV Products	15x15x10	5x5	2.85	2.50	140.30

For each event (laser pulse), we captured 10 waveforms from all 9 pixels (a central pixel plus 8 neighbors) and the cathode. The scan area was selected to ensure that the central pixel has the strongest signal, meaning that we covered the actual area of the central pixel. The boundaries of this area are not necessarily matched to the geometrical pixel boundaries because of the local non-uniformity of the electric field. After the carriers reach the anodes (collected by one or several pixels), all the waveforms plateau at either a close-to-zero level (if no charge has been collected at these pixels) or at some positive level proportional to the amount of collected charges (charge sharing). Using these levels we can identify the charge sharing versus single-pixel events and locate the actual physical boundaries between the neighboring pixels, i.e., when the levels measured from two adjacent pixels are equal. We also performed linear scans across the middle of the 3 pixels along the *X* and *Y* directions.

3. Data Analysis

For each beam position we captured 500 sequential waveforms and evaluated their X-Y coordinates using the time-correlated sample amplitudes from the recorded waveforms. For each coordinate, we selected two time-correlated samples: A_x^1 and A_x^2 for *X* and A_y^1 and A_y^2 for *Y* from the corresponding waveforms. Each pair was selected at a time at which the sample was the highest. In other words, one of A_x^1 and A_x^2 (and similarly of A_y^1 and A_y^2) is the maximum sample of the two corresponding waveforms. By selecting the highest amplitude of the time-correlated samples, we minimize the statistical (electronic) noise. As previously demonstrated [11] in our evaluation of one single pixel size (1.72) this gives the highest variation range, so we can expect to achieve the best position resolution.

As an example, Figure 1 shows scans at three different energies for the largest pixel-size detector tested (eV Products, Inc., 15x15x10 mm^3 volume and 2.85-mm pixel size). Each broad line consists of the overlapping Gaussian-like distribution of the estimated locations for each position of the laser beam. The FWHM of these distributions were used to estimate the position resolution at specific amounts of injected carriers. The amount of the locally injected carriers depends on the cathode contact and surface properties. The varying widths of the beam images display the different amounts of charge injected along the beam pass.

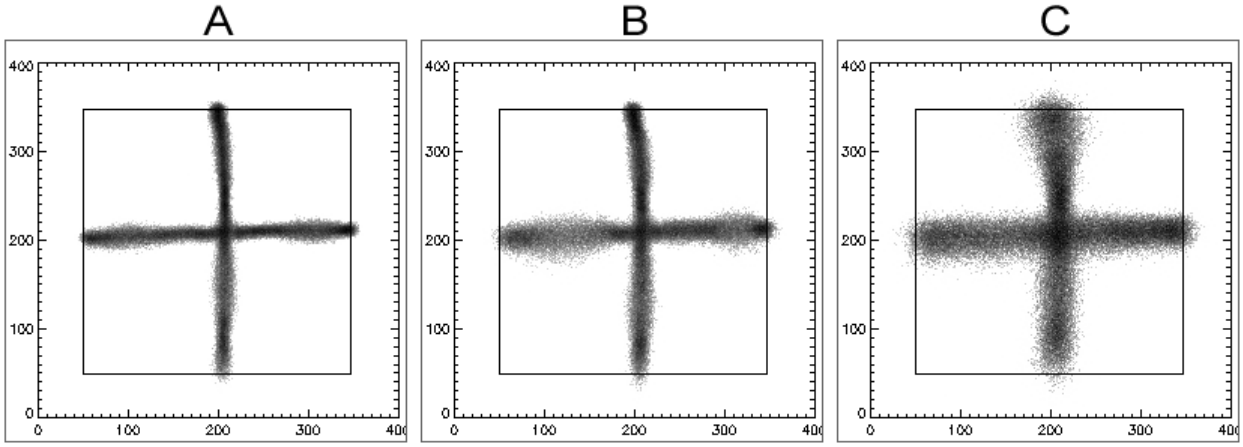

Figure 1. Position resolution evaluation of a 2.8-mm pixel size eV Products detector for three different energies. The line width gives the position resolution, which is estimated to be (a) 100 μm for an energy corresponding to 2 MeV. The resolution (b) is ~128 μm for a corresponding energy of 1.2-MeV, and (c) approximately 237 μm for a corresponding energy of 400 keV.

4. Results and Discussion

Fig. 2 shows the dependencies of the spatial resolution, % FWHM, on the amount of injected charge (converted into the deposited energy equivalents) for different pixel sizes. As previously mentioned, we used a ^{137}Cs source to convert the signal amplitudes into the deposited energies, and based on geometrical consideration, the position resolution scales proportionally to the pixel sizes. The amplitudes of the signals induced on the adjacent pixels increase with larger pixel areas resulting in a higher signal-to-noise ratio. One could expect that the position resolution reaches a minimum at a certain pixel size. However, as seen from the plot, the largest pixel size (2.8 mm) yields a poor position resolution compared to the smaller pixel sizes. A high signal-to-noise ratio impacts the

recorded waveforms and the amplitudes from the anodes, which affect the time-correlation technique and the position resolution. A small pixel size is affected by electron-cloud diffusion and electrostatic repulsion of the electrons, which alters the electron cloud before it reaches the anodes, whereas a large pixel size minimizes charge-sharing events.

Comparing the 1.72-mm and 1.4-mm pixel detectors with a corresponding nominal pixel size of 1.22 mm and 1.12 mm respectively, shows a difference of 0.10 mm. However, this 0.10-mm difference presents a higher spatial resolution of approximately 35 µm which becomes more apparent at the lower energies. We note that although the smaller pixel size presents the highest spatial resolution, it is also the smallest crystal at 10x10x10 mm^3. An 11x11 grid requires a higher number of readout channels, which presents a challenge for the application specific integrated circuit (ASIC). An even smaller pixel size would be heavily affected by charge-sharing events and diffusion as previously discussed.

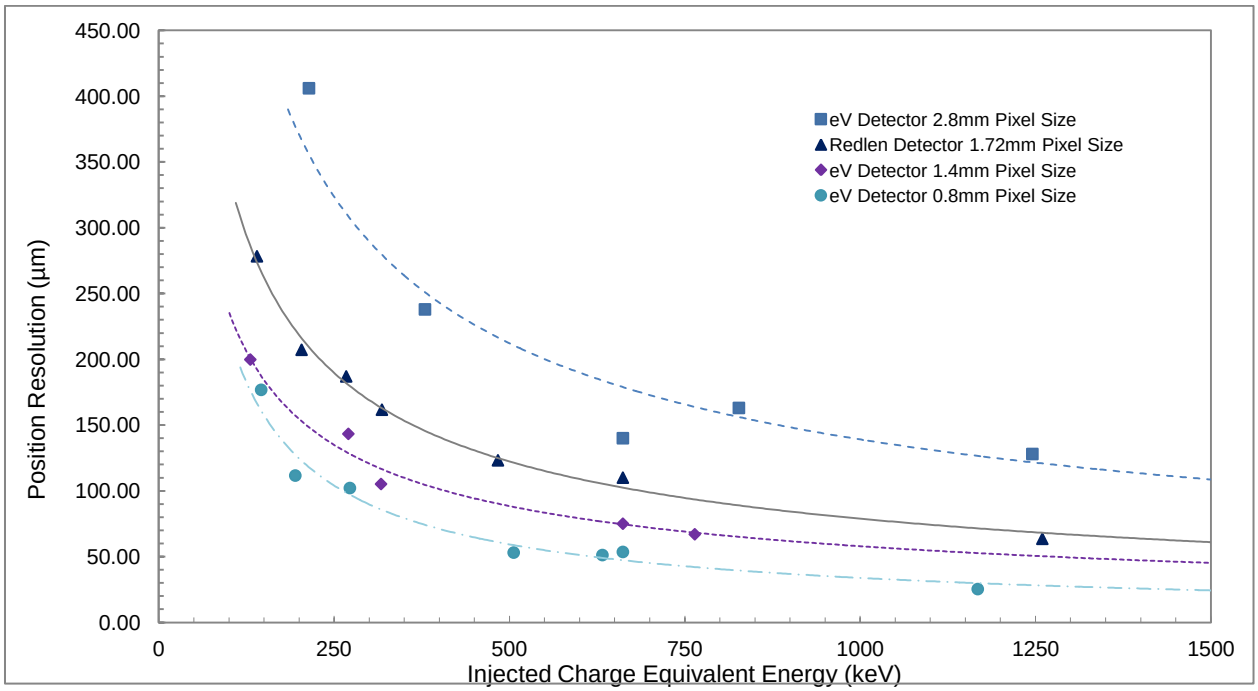

Figure 2. Position-resolution evaluation measurements at various gamma energies for all four pixelated detectors.

Fig. 3 illustrates an application of the 3D corrections to improve the spectral response measured from a representative pixel of a 20x20x5 mm^3 detector with a pixel size of 1.72 mm. The detector was irradiated with an uncollimated ^{137}Cs source. To reduce a number of stored waveforms, we used a high threshold to remove low-energy Compton events. In these measurements, we read only 10 signals. We could apply the correction technique to the area over a single selected pixel, and we could repeat the measurements for each selected pattern. The Z position determination is carried out by measuring the drift time directly from the waveforms [12]. This information allowed us to virtually divide the detector's volume (in this case the volume associated with one representative pixel) into a large number of small voxels and selectively apply a small scaling correction to the signal amplitudes captured from the individual voxels. The 3D lookup matrix with scaling coefficients was generated once for each detector prior to its use. This is done by aligning the photopeaks in the ^{137}Cs spectra acquired from each voxel during a calibration. In this case, we used 10x10x10 voxels. As seen, the energy resolution improves from about 2% FWHM at 662 keV down to 1.6% after the drift-time (1D) correction and to 1.0% after the 3D corrections, accordingly.

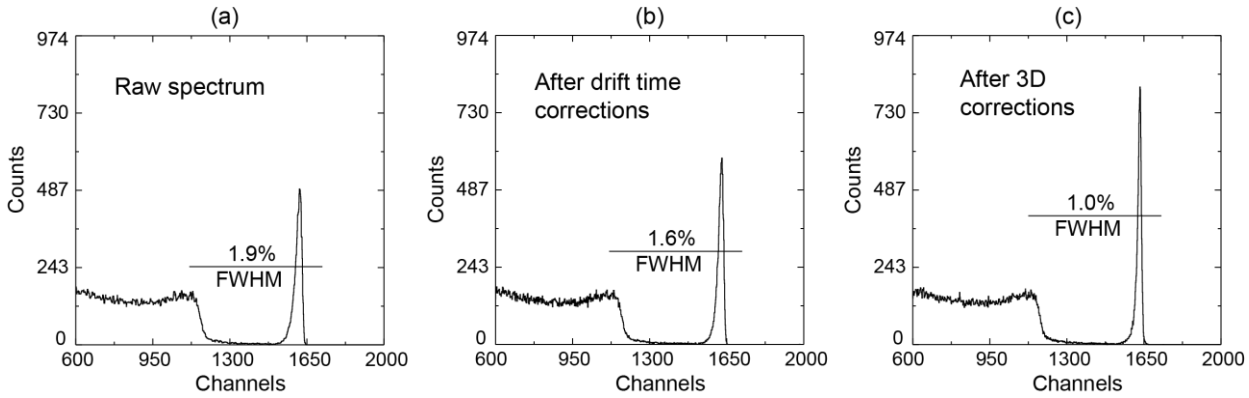

Figure 3. (a) Shows the raw ^{137}Cs spectrum measured from a representative pixel. Only single-pixel charge collection events were selected. (b) Shows the same spectrum after applying the drift-time (or Z-correction). As seen, a relative FWHM of the photopeak has improved from 1.9% down to 1.6%. After applying the 3D corrections (employing the time-correlated samples from adjacent pixels to evaluate X-Y coordinates), we achieved 1.0%. (c) The electronic noise evaluated using the baseline of the waveforms was ~3-4 keV or ~0.6% HWHM at 662 keV. We note that different data files were used for the voxels calibration and for presenting the results.

The detector selected for these demonstration measurements (supplied by eV Products, Inc.) was made from a CZT crystal grown by the High-Pressure Bridgman method (HPB) [13]. CZT crystals grown by this manufacturer typically have a very high mu-tau product, $>10^{-2}$ cm^2/V, but suffer from Tellurium (Te) inclusions whose diameters can exceed 30 µm. Te inclusions are the main cause of response non-uniformity in HPB-grown spectroscopy grade CZT crystals, which is difficult to correct because of the very small scale of response variations and their cumulative effect, which increases proportionally to the electron cloud drift distance. In this experiment, we have chosen the 5-mm-thick detector to reduce the latter effect. Segmenting the area into a smaller number of sub-pixels did not improve the energy resolution, since we reached the limit of the position resolution as demonstrated in Fig. 1. However, further improving the electronic noise (e.g., making a detector/ASIC hybrid) will make it possible to achieve better position resolution at 662 keV and, respectively, a finer segmentation.

5. Conclusion

Finding an optimal pixel size to maximize the position resolution, while mitigating the electronic noise, signal amplitude loss, charge-sharing events and electron-cloud diffusion, continues to be an ongoing effort. We investigated the position resolution of commercial pixelated detectors with standard patterns of varying pixel sizes (0.8 mm, 1.4 mm, 1.72 mm, and 2.85 mm) and illustrated the application of the response corrections in a pixelated detector. Our results indicate that a smaller pixel size yields a higher position resolution. However this requires a larger number of readout channels and thus poses a challenge for the data processing and heating dissipation. Increasing the pixel size to 1.12 mm (nominal) results in a reduction in position resolution of approximately 30 µm for low and high energies from the smallest pixel size (0.8 mm). Furthermore, increasing the nominal pixel another 0.10 mm will result in a further reduction of position resolution of ~30 µm. It is important to note that transient signals allow us to treat charge-sharing and single-point interaction events the same way. However, using a more accurate response function or applying geometrical corrections will lead to further improvement of the position resolution for all evaluated pixel sizes. We should note that results with a pulsed laser beam cannot substitute those with gamma-rays and in the latter case the resolution is expected to degrade further. Applying corrections yield an increase in the spectral resolution that varies depending on the quality of the crystal, but the presented results show an improvement of 0.9% FWHM. Further testing is needed to continue improving the 3D corrections in pixelated detectors.

Acknowledgements

This work was supported by U. S. Department of Energy, Office of Defense Nuclear Nonproliferation Research & Development (DNN R&D), and BNL's Technology Maturation Award. The manuscript has been authored by Brookhaven Science Associates, LLC under Contract No. DE-AC02-98CH1-886 with the U. S. Department of Energy.

Special thanks to The National GEM Consortium and the Alfred P. Sloan foundation MPhD Program. The authors wish to thank all the Brookhaven National Laboratory summer students who participated in taking these measurements. We also wish to thank Michael Spicer for his help coding in python.

References

[1] G. F. Knoll, Radiation Detection and Measurement, 3rd ed. 2000, New York: John Wiley & Sons, Inc.

[2] Z. He, W. Li, G. F. Knoll, D. K. Wehe, J. Berry, and C. M. Stahle, "3-D position sensitive CdZnTe gamma-ray spectrometers," Nucl. Instr. and Meth. A 422, pp. 173-178, 1999.

[3] A. E. Bolotnikov, G. S. Camarda, Y. Cui, G. De Geronimo, J. Eger, A. Emerick, J. Fried, A. Hossain, U. Roy, C. Salwen, S. Soldner, E. Vernon, G. Yang and R. B. James, "Use of high-granularity CdZnTe pixelated detectors to correct response non-uniformities caused by defects in crystals," Nucl. Instr. and Meth. A 805, pp. 41-54, 2016.

[4] W. Warburton, "An approach to sub-pixel spatial resolution in room temperature X-ray detector arrays with good energy resolution," In: Proceedings of Materials Research Society Symposium, 1997, vol. 487, pp. 531–536.

[5] M. A. J. van Pamelen and C. Budtz-Jørgensen, "CdZnTe drift detector with correction for hole trapping", Nucl. Instr. and Meth. A 411, pp. 197-200, 1998.

[6] T. Narita, J. E. Grindlay, J. Hong, F. C. Niestemski, Proc. SPIE, Vol. 5165, X-Ray and Gamma-Ray Instrumentation for Astronomy XIII, pp. 542-643, 2004.

[7] I. Kuvvetli, C. Budtz-Jørgensen, E. Caroli, N. Auricchio, Nucl. Instr. and Meth. A 624 (2010) 486.

[8] Y. Zhu, S. Anderson and Z. He, "Sub-Pixel Position Sensing for Pixelated, 3-D Position Sensitive, Wide Band-Gap, Semiconductor, Gamma-Ray Detectors," IEEE Transactions on Nuclear Science 58, no. 3, pp. 1400-1409, 2011.

[9] G. Montemont, S. Lux, O. Monnet, S. Stanchina, L. Verger, "Studying Spatial Resolution of CZT Detectors Using Sub-Pixel Positioning for SPECT," IEEE Trans. Nucl. Sci. 61, no. 5, pp. 2559–2566, 2014.

[10] C. Budtz-Jørgensen and I. Kuvvetli, "New Position Algorithms for the 3D CZT Drift Detector," IEEE Trans. Nucl. Sci., vol.64, no. 6, pp. 1611-1618, June 2017.

[11] L. Ocampo Giraldo, A.E. Bolotnikov, G.S. Camarda, S. Cheng, G. De Geronimo, A. McGilloway, J. Fried, D. Hodges, A. Hossain, K. Ünlü, M. Petryk, V. Vidal, E. Vernon, G. Yang, R.B. James, "Using a pulsed laser beam to investigate the feasibility of sub-pixel position resolution with time-correlated transient signals in 3D pixelated CdZnTe detectors," Nucl. Instr. and Meth. A 867, pp 7-14, 2017.

[12] A. E. Bolotnikov, G. S. Camarda, G. A. Carini, M. Fiederle, L. Li, G. W. Wright, and R. B. James, "Performance studies of CdZnTe detector by using a pulse-shape analysis" in Proc. SPIE, Hard X-Ray and Gamma-Ray Detector Physics VII, Bellingham, WA, 59200K-1 (2005).

[13] C. Szeles, "Advances in the Crystal Growth and Device Fabrication Technology of CdZnTe Room Temperature Radiation Detectors", IEEE Trans. Nucl. Sci. 51, no. 3, pp. 1242-1249, 2004.